Atomistic Simulations of Nanoindentation on Cu (111) with a Void
具孔隙（111）銅之奈米壓痕模擬

Chung-Ming Tan[1], Wei-Sheng Chen[1]
譚仲明 [1] ，陳幃盛 [1]
[1]Graduate School of OptoMechatronics and Materials，Wufeng University
[1] 吳鳳科技大學光機電暨材料研究所
email:cmtan@mail.wfc.edu.tw

Abstract：This paper employs static atomistic simulations to investigate the effect of a void on the nanoindentation of Cu(111). The simulations minimize the potential energy of the complete system via finite element formulation to identify the equilibrium configuration of any deformed state. The size and depth of the void are treated as two variable parameters. The numerical results reveal that the void disappears when the indentation depth is sufficiently large. A stress concentration is observed at the internal surface of the void in all simulations cases. The results indicate that the presence of a void has a significant influence on the nanohardness extracted from the nanoindentation tests.

Keywords: Nanoindentation, void, hardness.

摘要：本文採用靜態的原子模擬，模擬具孔隙銅 （111）的壓痕實驗。模擬是利用最小化系統的能量，通過有限元素公式來確定任何變形狀態之力平衡位置。大小和孔隙的深度被視為兩個可變參數。數值結果顯示，當壓痕深度充分大的時候孔隙消失。所有孔隙模擬案件均觀察到內表面的應力集中現象。結果表明，存在一個孔隙對奈米壓痕試驗測得之奈米硬度有重大影響。

關鍵字：奈米壓痕，孔隙，硬度

Introduction

Nanoindentation has evolved into a valuable means for determining mechanical properties of thin films and surfaces in nanometer regime [1-4]. Computer simulation has attracted an increasing interest as a means to gain insight into the atomic processes involved in nanoindentation [5-8]. Some previous studies have pointed out the indentation size effect for metals, wherein the hardness is reported to increase with decreasing indentation depth, especially in the sub-micrometer regime [9-14]. A literature review reveals that previous studies have never addressed the nanoindentation of voided

crystals. Although it is well known that even the purest real material contains a large number of defects within its crystal structure, it is impractical to simulate all of these defects at the atomic level. Hence, this study analyzes the interesting and computationally more straightforward problem of how the nanoindentation of Cu (111) crystal is influenced by the presence of a single void. The relative influences of the void size and void depth upon the extracted nanohardness results are explored and discussed.

Methodology

As shown in Figure 1, the simulated system configuration comprises a perfect three-dimensional crystalline slab of copper atoms with a (111) surface, and a spherical indenter whose outer surface atoms form many facets due to its crystalline structure. Although, not evident in the figure, the model also includes a spherical void embedded under the surface of the crystalline

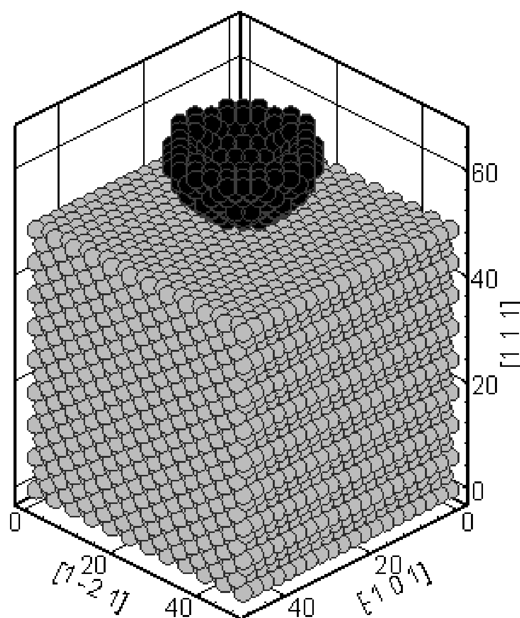

Figure1 The atomistic model used in the nanoindentation simulation. (unit:angstrom)

Cu slab directly beneath the tip of the indenter. The number of atoms in this study is 9948. The simulation assumes the indenter to have a diamond tip so hard compared with the copper thin film that indenter deformation could be neglected during the indentation process. Simulation boundary conditions assume the atoms at four sides and the bottom of the simulated film are fully constrained. The Sutton-Chen potential is employed as the interatomic potential of the copper substrate in this study. It has the following form:

$$U = \sum_i U_i \tag{1}$$

$$U_i = \varepsilon\left(\frac{1}{2}\sum_{j\neq i}\left(\frac{a}{r_{ij}}\right)^n - c\sqrt{\rho_i}\right) \tag{2}$$

Here ρ_i is an electron density-like term for atom i as follows:

$$\rho_i = \sum_{j\neq i}\left(\frac{a}{r_{ij}}\right)^m \tag{3}$$

where r_{ij} is the distance between atoms i and j, while copper constants ε, a, c, m, and n are 1.238×10^{-2}, 3.6, 39.432, 6, and 9, respectively. The potential between carbon and copper atoms used in the simulation is the Born-Mayer potential, which produces only impulsive force. It has the form

$$\phi(r_{ij}) = A \exp[-2\alpha(r_{ij} - r_0)] \tag{4}$$

where r_{ij} is the distance between carbon atom i and copper atom j, and carbon/copper constants A, a and r_o are, respectively, 0.3579, 0.9545 and 2.5.

Nanoindentation is simulated as moving the indenter downward incrementally to impress the copper substrate. Every time the indenter moves downward a displacement increment, the energy of the whole system is minimized to achieve the equilibrium. Energy minimization algorithm used in this study is the block-diagonal Newton-Raphson method. In this study, we have simulated three spherical indenter and pyramidal indenter nanoindentation cycles of which maximum indentation depths are $4\overset{o}{A}$, $7\overset{o}{A}$, and $10\overset{o}{A}$. The curves of load (force experienced by the indenter) versus indentation depth for these cases are recorded. It can be seen that every indentation cycle recorded represents hysteretic loop, i.e. there are plastic deformations occurred in the loading processes. In this study, the stability of a crystalline structure is correlated to and can be monitored by the positiveness of the Hessian matrix. The irreversible plastic deformations observed in the simulation can be considered to be consequences of change of the crystalline structure due to instabilities induced by localized high stress.

Result and Discussion

In this work, we first use the contact pressure to identify the true contact area at full load in the simulations. Once we have the true contact area, the nanohardness can be computed from the load divided by the projected area of contact at that load. Having evaluated the contact pressure, the true contact area can be accurately determined and the

nanohardness can be obtained. Table 1 lists the maximum loads and nanohardnesses obtained for the different void parameters considered in the present simulations.

The nanohardness is computed by dividing the maximum load by the projected area of contact at that load. Table 1 demonstrates that a larger maximum load always corresponds to a larger nanohardness for the current simulation conditions. Hence, it can be concluded that the contact area is not influenced significantly by the presence of a void.

Table 1. Nanohardness values for two void parameters (Void Size and Depth).

Void parameters (Size and Depth)	Maximum Load (10 eV/nm)	Nano-hardness (Gpa)
No Void	222	6.27
Size=0.8 nm Depth=1.3 nm	194	5.58
Size=1.2 nm Depth=1.0 nm	183	5.32
Size=1.2 nm Depth=1.5 nm	190	5.52
Size=1.2 nm Depth=2.0 nm	196	5.69
Size=1.6 nm Depth=1.7 nm	182	5.29

Figure 2 shows the distributions of the hydrostatic stress and the von Mises stress induced at the maximum indentation depth in the cross-section of the indented copper substrate through the indenter tip and parallel with the (-1 01) plane. The results correspond to the case of no void and to the case of a void with a diameter of 1.2 nm and a depth of 1.5 nm. A comparison of the four subplots reveals that the distribution of the von Mises stress is not affected significantly by the presence of a void. However, the void does have a significant influence on the distribution of the hydrostatic stress. It can be seen that the stress accumulates at the internal surface of the void causing a reduction in the contact pressure.

Figure 3 presents the distributions of the hydrostatic stress for two different void parameters in the same cross section as shown in Figure 3. Subplots (a)~(c) reveal the variation of the hydrostatic stress distribution with the void size, while subplots (d)~(f) illustrate the variation of the hydrostatic stress distribution with the void depth. It is observed in subplots (a) and (d) that although the void disappears, a stress concentration remains at the original void location. The disappearance of the void is to be expected since

in these two cases, the indentation depth is sufficiently large to cause many surrounding atoms to slip into the void vacancy. The remaining

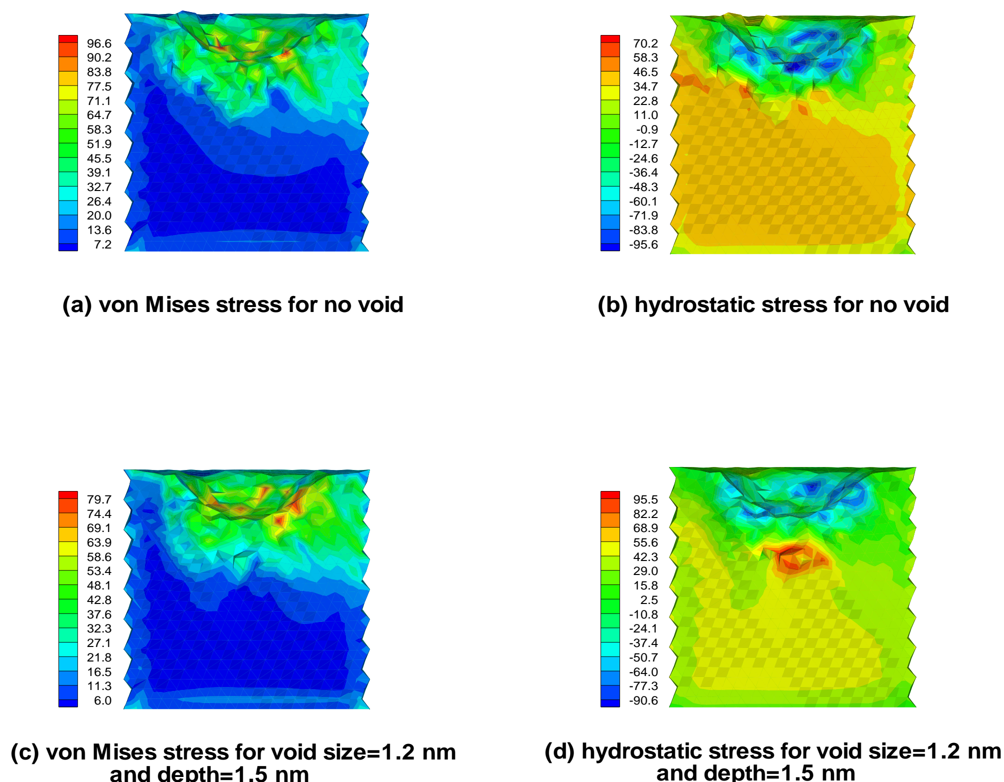

Figure 2. Distributions of hydrostatic stress and von Mises stress in cross-section through indenter and parallel with (-1 01) plane: (a) von Mises stress for no void. (b) hydrostatic stress for no void. (c) von Mises stress for void size=1.2 nm and depth=1.5 nm. (d) hydrostatic stress for void size=1.2 nm and depth=1.5 nm. (Stress unit: Gpa)

subplots of Figure 3 all reveal that stress accumulates at the internal surface of the void. The stress accumulation causes a reduction in the contact pressure and prompts the void to deform into an elliptical shape. A stress reduction in the contact area is consistent with the maximum load reduction observed when a void exists in the substrate.

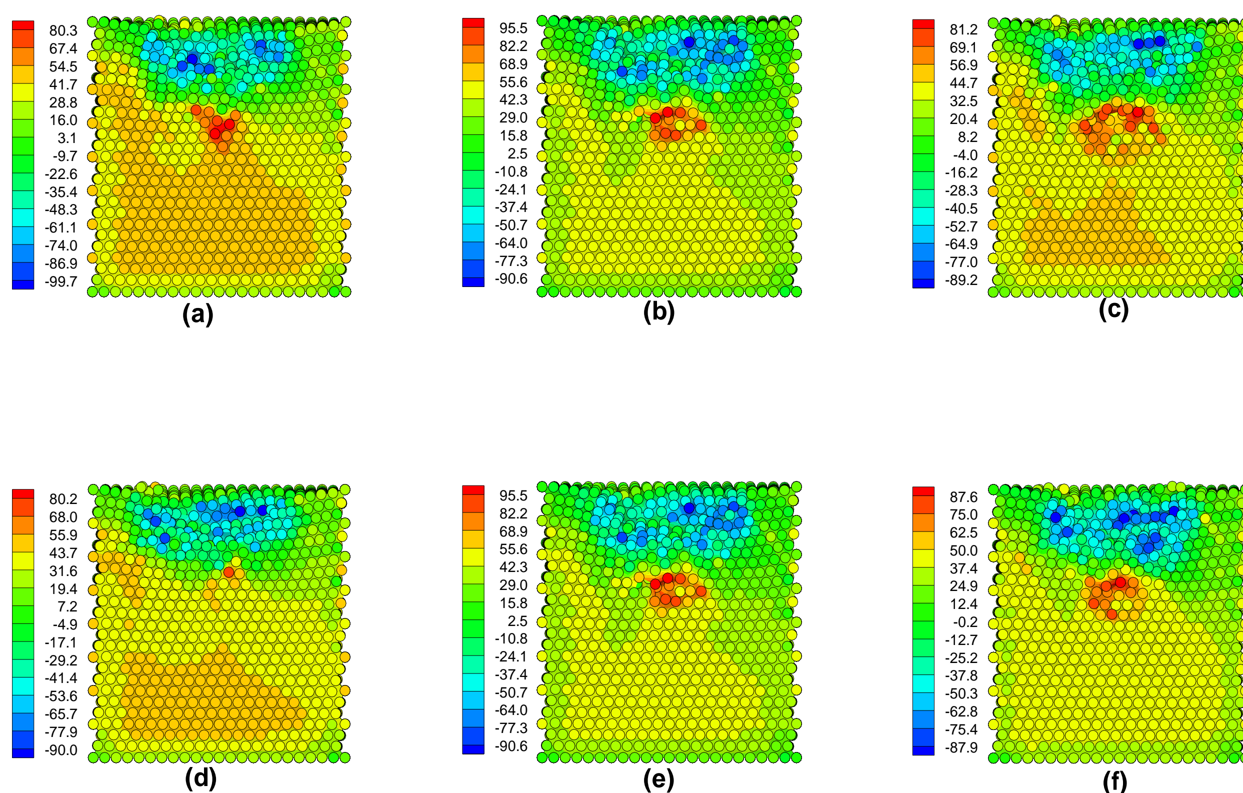

Figure 3 Variation of hydrostatic stress distribution in cross-section through indenter tip with two void parameters: (a)~(c) void size=0.8, 1.2, and 1.5 nm. (d)~(f) void depth=1.0, 1.5, and 2.0 nm.

In conclusion, stress analysis has explained the observed reduction in maximum load caused by a void and that the contact area is unaffected by the existence of a void. However, the cases simulated in this study have revealed that the existence of a void causes a reduction in the magnitude of the nanohardness of the order of approximately 10~15 %.

References

[1] B. N. Lucas, W. C. Oliver, and J. E. Swindeman, Mat. Res. Soc. Symp. Proc. **522**, 3 (1998)

[2] J. L. Hay, M. E. O'Hern, and W. C. Oliver, Mat. Res. Soc. Symp. Proc. **522**, 27 (1998)

[3] J. C. Hay, and G. M. Pharr, Mat. Res. Soc. Symp. Proc. **522**, 39 (1998)

[4] W. Lu, and K. Komvopoulos, J. Tribo. **123**, 641 (2001)

[5] R. Perez, M. C. Payne, and A. D. Simpson, Phys. Rev. Lett. **75**, 4748 (1995)

[6] J. A. Zimmerman, C. L. Kelchner, P. A. Klein, J. C. Hamilton, and S. M. Foiles, Phys. Rev. Lett. **87**, 165507-1 (2001)

[7] O. R. de la Fuente, J. A. Zimmerman, M. A. Gonzalez, J. de la Figuera, J. C. Hamilton, W. W. Pai, and J. M. Rojo, Phys. Rev. Lett. **88**, 036101-1 (2002)

[8] J. Knap and M. Ortiz, Phys. Rev. Lett. **90**, 226102-1 (2003)

[9] W. D. Nix and H. Gao, J. Mech. Phys. Solids **46**, 411 (1998)

[10] H. Gao, Y. Huang, W. D. Nix, and J. W. Hutchinson, J. Mech. Phys. Solids **47**, 1239 (1999)

[11] Y. Huang, H. Gao, W. D. Nix, and Z. C. Xia, J. Mater. Res. **8**, 1786 (2000)

[12] K. C. Hwang, H. Jiang, Y. Huang, H. Gao, and N. Hu, J. Mech. Phys. Solids **50**, 81 (2002)

[13] A. A. Elmustafa and D. S. Stone, J. Mech. Phys. Solids **51**, 357 (2003)

[14] K. C. Hwang, H. Jiang, Y. Huang, and H. Gao, Int. J. Plast. **19**, 235 (2003)